

A NEW METHOD TO MEASURE WATER, OIL AND GAS SATURATION PROFILES IN THREE-PHASE GAS INJECTION

O. VIZIKA and F. KALAYDJIAN
Institut Francais du Pétrole

Abstract

In the present paper an original method is presented to acquire simultaneously water, oil and gas saturation profiles as a function of time in tertiary gravity assisted gas injection. The method consists in combining local electrical resistivity and γ -ray attenuation measurements. Resistivity measurements give the local water saturation whereas the oil and gas saturations are calculated based on the γ -ray attenuation profiles. The method has been applied to measure three-phase local saturations during gravity assisted gas injection experiments in water-wet sandpacks; in these experiments the ability of oil to form films on water in presence of gas, that is characterised by the spreading coefficient, was investigated.

The results are in very good agreement with local saturation CT-scanner measurements and with bulk saturations obtained by continuous weighing of the recovered fluids. As a validation of the method the oil relative permeability is calculated, based on the evolution of the saturation profiles and it is used to simulate the experiments. A good numerical description of the experimental behavior is obtained. Throughout the same experiments it is proved that the spreading coefficient plays a major role on the fluid distribution and recovery efficiency in tertiary gravity assisted gas injection e.g. when water is mobile.

Introduction

Massive gas injection under secondary and mainly under tertiary conditions is increasingly being considered as a very efficient oil recovery process. When applied in rather permeable reservoirs and assisted by gravity forces, very low residual oil saturations are observed⁵. It is of prime interest to be able to predict reachable recovery in a given period of time by calculating the relative permeabilities especially at these low saturations where flow of oil by film predominates. To do so, measurement of the three-phase saturation profiles and their evolution with time is needed. To obtain three-phase saturation profiles different methods have been used in the past, as double energy CT-scanner measurements³, dual-energy gamma attenuation measurements², or doping of water and oil with two different radioactive compounds⁴. The two first methods are rather difficult to set up while the latter may be dangerous and not easy to implement.

In this paper a new method is presented to acquire simultaneously water, oil and gas saturation profiles during a gas injection. Electrical resistivity measurements along the porous medium permit to obtain the water distribution, while the gas and oil saturation profiles are calculated based on the γ -ray attenuation profiles.

The paper consists of two parts. In the first part the method and the experimental set-up are presented along with the calculations and considerations to derive the three-phase

saturation profiles. In the second part a validation of the method is provided by applying it to the study of three phase distribution for a tertiary gravity assisted gas injection e.g. with mobile water. Two different cases are considered, one with a positive and one with a negative spreading coefficient. The spreading coefficient, defined as $S = \gamma_{wg} - (\gamma_{wo} + \gamma_{og})$, quantifies the liquid-liquid interactions that have been seen to play a determining role on the efficiency of secondary and tertiary gravity assisted gas injection^{3,10}. The spreading coefficient has been also shown to affect the capillary pressure curve⁶ and the relative permeabilities⁷. When it is positive the oil phase spreads over water in presence of gas to form a film. These films, called *spreading films*, maintain the hydraulic continuity of the oil which can drain down to low residual saturations¹⁰. Three-phase oil relative permeabilities are calculated from the saturation profile evolution and they are used to simulate the experiments.

Method Description - Experimental Set-Up

Electrical resistivity measurements

Deducing fluid saturations from electrical resistivity data is a rather old idea. It is extensively used to calculate the water saturation from the wireline resistivity log when the resistivity of the rock as a function of water and oil saturation is known. The best way to do so is by measurement of the resistivity index of the porous medium. The resistivity index is defined as the ratio of the resistivity of partially over the resistivity of fully saturated with brine rock¹;

$$I_R = R_t/R_0 \quad (1)$$

To calculate the saturation when the resistivity is known the following empirical correlation first proposed by Archie¹ is used;

$$I_R = S_w^{-n} \quad (2)$$

where S_w is the brine saturation and n is called the saturation exponent. For strongly water-wet porous media (sandpacks) the above formula represents usually successfully experimental data⁹ for n close to 2. In the present paper electrical resistivity measurements are used to obtain the water saturation profile, while the oil and gas local saturations are deduced from γ -ray attenuation measurements as explained below.

Gamma ray attenuation measurements

Local saturation calculations from γ -ray attenuation measurements are based on Beer-Lambert's law that relates the number of incident photons, N_0 , to the number of the transmitted photons, N , through a body with thickness l as follows;

$$N = N_0 e^{-\mu l} \quad (3)$$

where μ is the linear absorption coefficient of the material. It is easily seen that for a porous material saturated with water, oil and gas the transmitted intensity as given as

$$N = N_0 e^{-[\mu_{pm}(1-\phi) + \mu_w S_w \phi + \mu_g S_g \phi + \mu_o(1 - S_g - S_w)\phi] l} \quad (4)$$

where ϕ is the porosity, S the local saturation and the subscripts pm, w, g, and o denote porous medium, water, gas and oil respectively. After some simple calculations the local gas saturation at each measurement point as a function of the initial water saturation profile obtained by γ -ray measurements (S_{win}) and the actual water saturation profile given by

resistivity measurements (S_w), is given by the following relation

$$S_g = \frac{(1 - S_w) \ln \frac{N_{wo}}{N_w} - (1 - S_{win}) \ln \frac{N}{N_w}}{(1 - S_{win}) \ln \frac{N_w}{N_g} + \ln \frac{N_{wo}}{N_w}} \quad (5)$$

where N_g , N_w , N_{wo} are the reference attenuation profiles of the porous medium saturated with gas, with water and with water/oil (at S_{win}) respectively.

Porous medium cell

A special cell has been designed and constructed to enable both resistivity and γ -ray attenuation measurements. The cell contains eight o-ring copper electrodes placed in equal

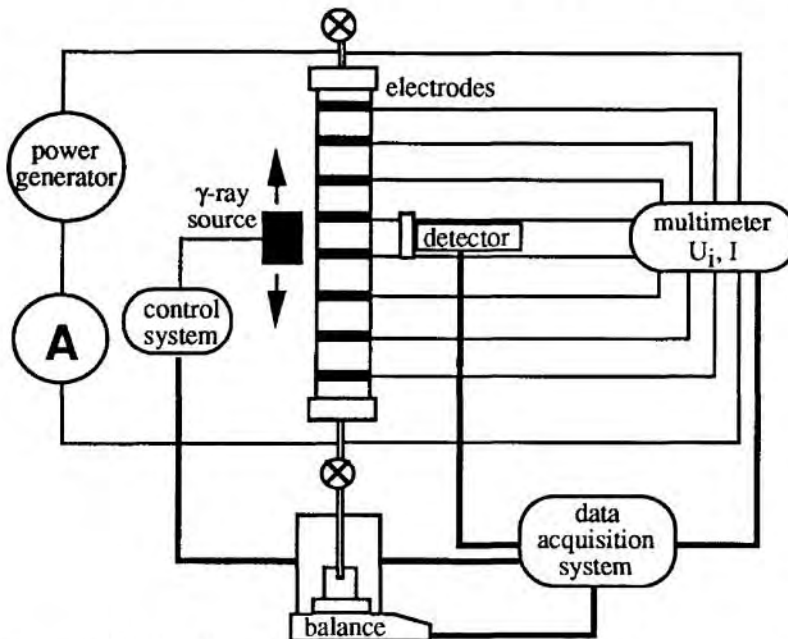


Figure 1: Schematic representation of the experimental set-up.

separations along the porous medium allowing the measurement of the electrical resistivity of each segment, and then calculation of the water saturation that is assumed homogeneous within the same segment. A schematic depiction of the experimental set-up is given in Figure 1. The Americium γ -ray source and the detector are vertically displaced by an automatically controlled translator system. A constant tension of several hundred of millivolts and a frequency of 300Hz is applied by the power generator in the two ends of the porous

Experimental procedure

The experimental procedure is as follows:

- At the beginning the porous medium is empty, dry and vertically positioned. A γ -ray attenuation profile gives N_g .
- Then water is introduced under vacuum to completely fill the sandpack. An electrical resistivity profile, giving R_0 , and a γ -ray attenuation profile (N_w) are necessary at this stage for calibration purposes. From the γ -ray attenuation profile, the porosity profile of the porous medium is deduced.
- Water then is displaced by oil down to irreducible water saturation, S_{wi} . The water/oil saturation profile is determined by the γ -ray technique (N_{wo}). The end point of the oil relative permeability curve ($K_{ro,max}$) is also measured. The electrical resistivity profile gives R_t and the exponent n is easily calculated from equations 1 and 2.

- The oil is displaced by water to obtain a residual oil saturation to waterflooding, S_{orw} . The water/oil saturation profile is determined by the γ -ray technique, and the relative permeability to water is also measured.
- The outlet valve is connected to the collection vessel, and both inlet and outlet valves are opened. As air enters the porous medium under constant pressure or constant flowrate conditions, the water and oil recovered are separated in a specially designed separator and their respective weights are continuously registered as a function of time. Electrical resistivity measurements and γ -ray attenuation measurements are continuously obtained and the saturation profiles of the three fluids are determined (equations 2 & 5). To obtain the γ -ray absorption measurement at one point an acquisition time of 100s is needed. The electrical resistivity profiles are considered to be obtained instantaneously.

Application: Tertiary Gravity Assisted Gas Injection

The method described above has been applied to deduce three-phase oil relative permeabilities from the saturation profile evolution in the case of a gravity assisted gas injection in strongly water-wet porous media. The spreading coefficient of oil on water in presence of gas has been chosen as the parameter to be studied, since it has been already seen that the spreading conditions affect both the recovery kinetics and the recovery efficiency. In terms of saturation profiles that means that both the local saturation evolution and its equilibrium value are expected to be highly influenced.

Porous medium - Fluids. The experiments have been performed in sandpicks with average grain size of $120\mu\text{m}$. The properties of the porous medium and the recovery data are given in Table 1. Water-wet conditions are obtained by thoroughly cleaning and rinsing the sand. The fluids are carefully chosen and prepared as described elsewhere¹⁰. Two water-oil-gas systems have been used in order to obtain a positive and a negative spreading coefficient. The physicochemical properties of the fluids are given in Table 2.

TABLE 1: PETROPHYSICAL PROPERTIES AND RECOVERY DATA

Experiment No	ϕ	K (D)	$K_{ro,max}$	$K_{rw,max}$	S_{wi}	S_{orw}	S_{org}	Recovery % OOIP
1	0.36	16.6	0.5	0.45	0.26	0.165	0.07	54
2	0.35	12.	0.4	0.62	0.24	0.126	0.11	13

TABLE 2. PHYSICOCHEMICAL PROPERTIES OF THE FLUID SYSTEMS

Fluid system	ρ_w Kg/m ³	ρ_o Kg/m ³	μ_w c p	μ_o c p	γ_{wg} mN/m	γ_{og} mN/m	γ_{ow} mN/m	S mN/m
Brine (30g/l NaCl)- Soltrol 170- Air	1019.	789.	1.05	2.75	71.	25.7	32.	+13
Brine (40g/l BaCl ₂) +3% i-butanol - Soltrol 170- Air	1021.	785.	1.12	2.75	40.6	26.3	16.4	-2

Results. a) Spreading conditions The fluid system consisted of brine (30g/l NaCl),

Soltrol 170 and air, and had a positive spreading coefficient $S=+13\text{mN/m}$. The irreducible water saturation profile has been measured with the γ -ray attenuation technique and by CT-scanner measurements and has been used to calibrate the electrical resistivity measurements. Both methods gave the same exponent $n=2.09$.

After gravity assisted gas injection has started, electrical resistivity and γ -ray attenuation profiles were periodically measured. The former have been used to calculate the water saturation profile by using equation 2, and its evolution with time. A sequence of those profiles is given in Figure 2. The latter has been used to calculate the oil and gas saturation profiles (Figure 3) by using equation 5. The error on the determination of the water saturation by resistivity measurements has been evaluated to be less than 3% and on the gas saturation less than 4.5%. It highly depends on the quality of the calibration curve. It can be seen that as gas enters the porous medium it displaces water first in the upper part of the sandpack down almost to its irreducible water saturation ($\approx 15\%$). Then oil starts getting displaced slowly and efficiently as it can be seen in Figure 3 and very low oil saturations are attained in the upper part of the porous medium ($\approx 5\%$).

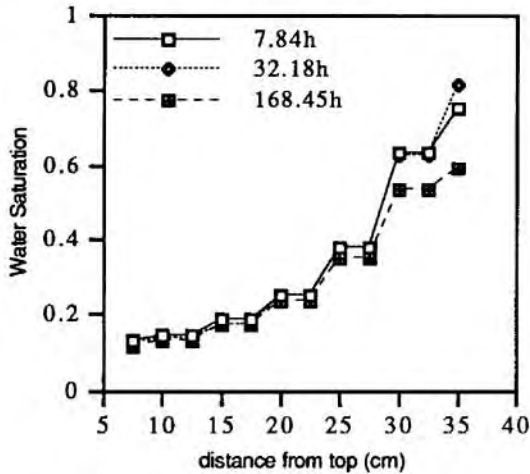


Figure 2: Water saturation profiles from electrical resistivity measurements

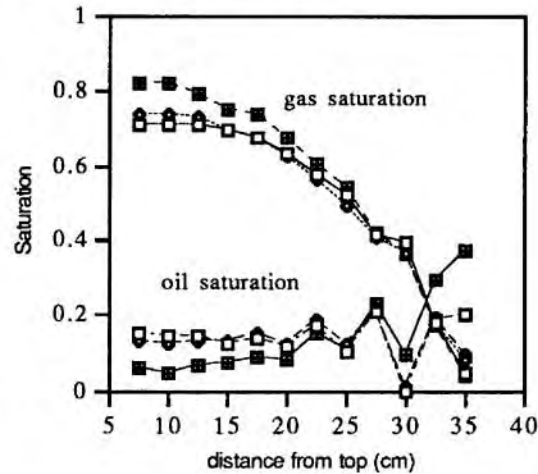


Figure 3: Gas and oil saturation profiles for the imposed pressure drop part of the experiment

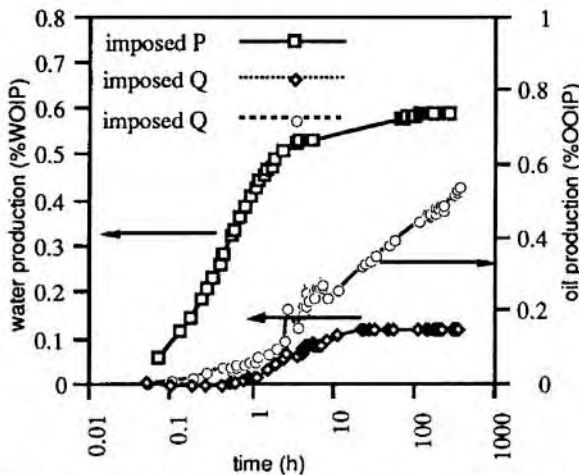


Figure 4: Oil and water recovery curves for spreading conditions

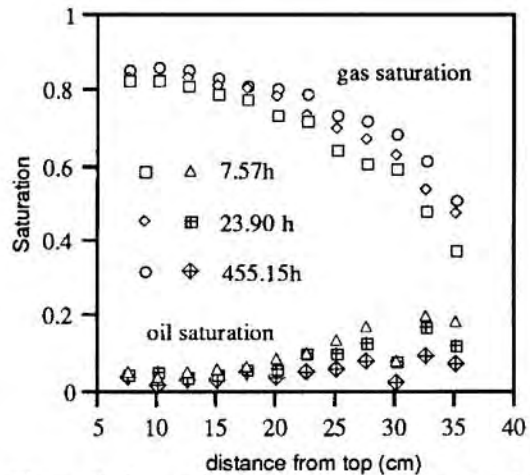


Figure 5: Gas and oil saturation profiles for the imposed gas flowrate part of the experiment

At the imposed pressure drop part of the experiment gas breakthrough did not occur and oil production has not been observed, only an oil accumulation towards the bottom of the porous medium has been detected. The recovery curve is given in Figure 4.

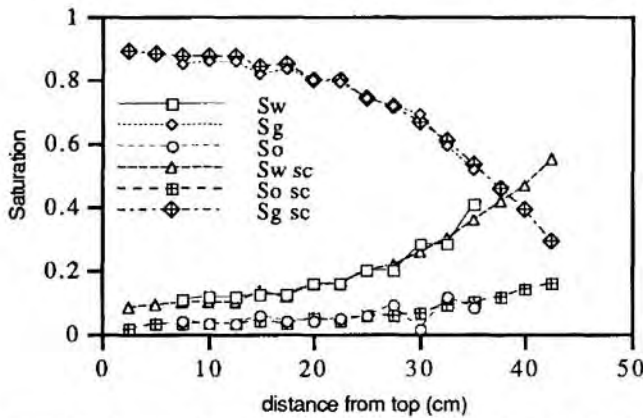


Figure 6: Comparison between the saturation profiles obtained with the present method and those measured with CT-scanner

those obtained at the final stage of the experiment by the combined resistivity/ γ -ray measurement method. The very good agreement obtained (Figure 6) ensures the reliability of the method proposed here at least in water-wet porous media. Calculated average saturations from the saturation profiles are also found to be in good agreement with bulk

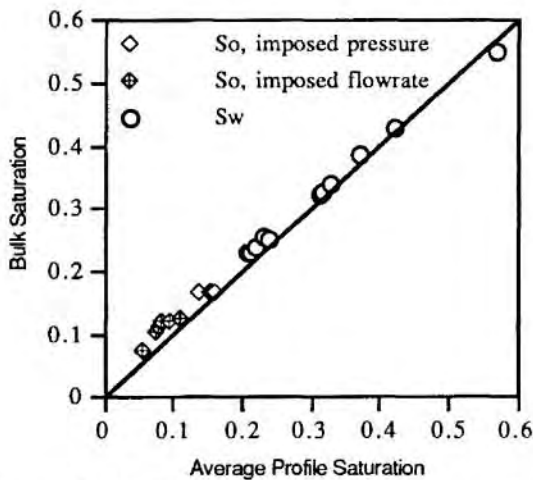


Figure 7: Water and oil bulk saturations against average saturations calculated from the profiles

measurements has served to calibrate the electrical resistivity measurements by calculating the exponent n ($n=2.14$). An imposed pressure drop gravity assisted gas injection has been operated followed by an imposed flowrate part as described above for spreading conditions. The recovery curve is given in Figure 8. During the imposed pressure drop experiment gas breakthrough did not occur and only water is produced. Water's recovery stops abruptly after having produced $\sim 58\%$ of water in place. Then a constant gas flowrate of 10ml/h is imposed and water production starts again giving in total another 15% of water in place.

Then the experiment continued by imposing a constant gas flowrate of 10ml/h. The water production restarts but oil comes also along and a slow and long oil recovery is obtained leading to a very low average oil saturation ($\sim 7\%$), while locally the residual oil saturation goes down to 2% as it can be seen from the saturation profiles (Figure 5). Gas breaks through at 4h from the beginning of the gas injection. At the end of the experiment the final water, oil and gas saturation profiles were measured with double energy CT-scanner and were compared to

saturations obtained by continuous weighing of the recovered fluids as it can be seen in Figure 7 where bulk water and oil saturations, calculated from the production data are plotted against the average profile saturations. Saturation profiles slightly underestimate the bulk values because they do not take into account liquid capillary retention that is rather pronounced in the very bottom of the porous medium.

b) Non-spreading conditions The fluid system consisted of brine (40g/l BaCl_2)+3% iso-butanol, Soltrol 170 and air; this system gives a negative spreading coefficient $S=-2\text{mN/m}$. Again the irreducible water saturation profile measured with the γ -ray attenuation technique and by CT-scanner

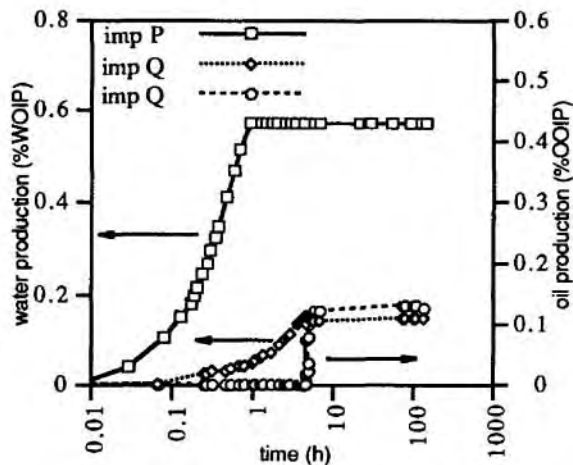


Figure 8: Oil and water recovery curves for non-spreading conditions

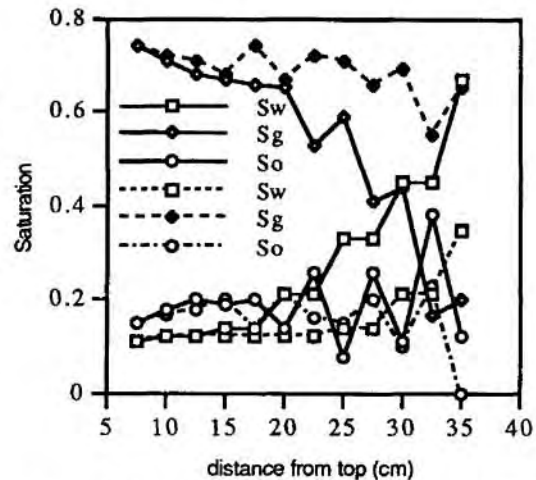


Figure 9: Saturation profiles for non-spreading conditions at the end of the pressure imposed (plain lines) and flowrate imposed (dashed lines) part of the experiment

Gas breakthrough time was higher than for spreading conditions (~ 4.7 h). Oil starts getting produced only almost four hours after the gas flowrate has been applied. However only a small quantity is rapidly produced, then the oil recovery curve attains the asymptote and the global residual oil saturation is stabilised to a rather high value ($S_{org} = 11\%$) much higher than for spreading conditions. The oil recovery (around 13%) is much poorer than for spreading conditions where 54% of oil originally in place is recovered.

The saturation profiles (Figure 9) show a slight accumulation of oil during the first part of the experiment, then during the imposed flowrate gas injection some oil gets produced but it comes only from the lower part of the porous medium. The oil trapped in the upper part does not get remobilized during the applied flowrate gas injection. Also locally the residual oil saturation is higher than for spreading conditions. The experiment has been duplicated and a very good reproducibility has been obtained in both recovery behavior and saturation profile measurements.

The differences obtained in the oil recovery kinetics and the displacement efficiency between spreading and non-spreading conditions can be explained on the basis of microscopic mechanisms. For $S > 0$, as gas contacts an oil blob surrounded by water, the oil forms spreading films on the water. As gas advances in the porous medium the gas-oil contacts are multiplied and they transform a small quantity of oil into films between water and gas. These films assure the hydraulic continuity of oil when gas breaks through (for the imposed flowrate injection); this continuous oil is constantly subjected to a pressure gradient due to gravity. Through the spreading films oil is easily though slowly recovered and the overall process efficiency is very high. For $S < 0$ these films are never formed and the oil phase remains disconnected. Furthermore oil ganglia block the larger pathways of the water-wet porous medium and consequently even water production is prohibited. When a gas flowrate is applied water production restarts. However oil is produced only several hours later, probably through a piston like displacement mechanism, this is why oil recovery stops shortly afterwards.

Discussion

Three-Phase Oil Relative Permeabilities

Relative permeabilities may be calculated by considering the flowrate (or rate of saturation change) past a measurement point, using Darcy's law and neglecting capillary effects⁴. For the vertical displacement of oil and gas Darcy's law gives for their respective velocities

$$U_o = -\frac{KK_{ro}}{\mu_o} \left(\frac{dP_o}{dz} - \rho_o g \right) \quad \text{and} \quad U_g = -\frac{KK_{rg}}{\mu_g} \left(\frac{dP_g}{dz} - \rho_g g \right) \quad (6)$$

If $dP_o/dz = dP_g/dz = \text{constant}$ or if capillary pressure is neglected ($P_g = P_o$) - and this is true far from the bottom of the porous medium and almost everywhere for the applied gas flowrate part of the experiment- and gas mobility is much higher than oil mobility, the above equations give

$$U_o = \frac{KK_{ro}}{\mu_o} (\rho_o - \rho_g) g \quad (7)$$

By combining the mass conservation equation for oil in the porous medium

$$\phi \frac{\partial S_o}{\partial t} + \frac{\partial U_o}{\partial z} = 0 \quad (8)$$

with equation 7, and integrating between the top of the core ($z=0$) and the measurement point z , the following formula for K_{ro} is obtained

$$K_{ro} = -\frac{\phi \mu_o}{K(\rho_o - \rho_g) g} \int_0^z \frac{\partial S_o}{\partial t} dz \quad (9)$$

The term $\partial S_o / \partial t$ is estimated from the evolution of the oil saturation profile with time at the different measurement points.

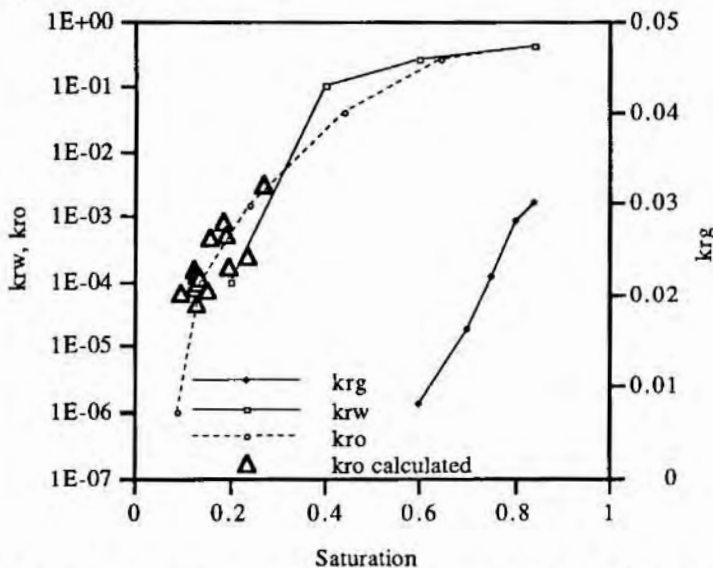


Figure 10: Gas, oil and water relative permeabilities as a function of their respective saturations. The points represent the calculated K_{ro} from the saturation profile evolution

The results appear in Figure 10 (points) along with the relative permeability curves that have been determined in order to best fit the experimentally obtained recovery curves as explained below. It is seen that very low values for the oil permeability are obtained, corresponding to the slow evolution of the oil profile throughout the whole gravity drainage experiment.

Numerical simulations

The experiment for spreading conditions has been simulated using a reservoir simulator (Σ CORE), which is a

multipurpose compositional reservoir simulator based on an up to three phases and three dimensions model. It has been jointly developed by French petroleum and gas companies

and the Institut Français du Pétrole. Three-phase relative permeabilities can be calculated from two-phase data or directly introduced in the data file in the form of tables where all three relative permeabilities depend on two saturations, that means on the distribution of the three fluids ($K_{ro}=f(S_w, S_g)$, $K_{rg}=f(S_w, S_g)$, $K_{rw}=f(S_w, S_g)$). In this study the second method has been used.

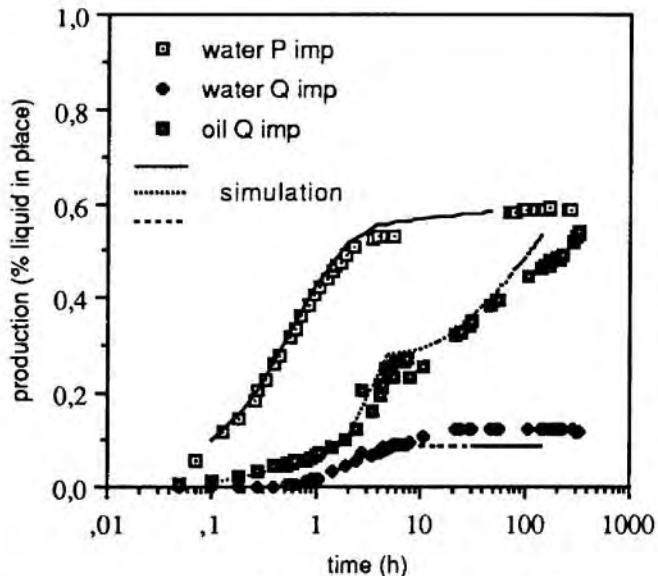


Figure 11: Experimental and simulated water and oil recovery curves for spreading conditions

This method permits to enter directly three-phase data obtained in the laboratory, instead of three-phase permeabilities calculated from two-phase data by using ill-justified models (e.g. Stone's models). The end point of the oil ($K_{ro,max}$) and the water ($K_{rw,max}$) relative permeability curves have been used as input in the simulator. The oil relative permeabilities calculated from the oil saturation profiles (Figure 10) have been used as input. The gas and water relative permeabilities have been adjusted in a way to give a good history match of the water and oil recovery curves. The results, presented in Figure 11, show a good fit of the experimental behavior. Also a reasonable fit of the saturation profiles is obtained, the discrepancies being due to the

uncertainty on the saturation measurements and on the local heterogeneities of the porous medium.

Conclusions

An original method to acquire simultaneously water, oil and gas saturation profiles as a function of time in tertiary gas injection by combining local electrical resistivity and γ -ray attenuation measurements has been presented.

The method has been applied to measure three-phase local saturations during gravity assisted gas injection experiments in water-wet sandpacks; in these experiments the ability of oil to form films on water in presence of gas was investigated.

The following conclusions can be deduced:

- 1 Calculated final saturation profiles are in good agreement with double energy CT-scanner measurements.
- 2 Calculated average saturations are in good agreement with bulk saturations obtained by continuous weighing of the recovered fluids.
- 3 The spreading coefficient plays a major role on the fluid distribution and recovery efficiency in tertiary gravity assisted gas injection by conditioning the formation of oil spreading films that only can lead to low oil saturations. The saturation profile measurement method presented in the present paper has been successfully applied for both spreading and non-spreading conditions.
- 4 Based on the saturation profiles three-phase relative permeabilities have been calculated and used to simulate the experiments.

Nomenclature

I_R	resistivity index	S_{win}	initial water saturation
K	permeability (m^2)	S_{org}	residual oil saturation (gas drainage)
K_r	relative permeability	S_{orw}	residual oil saturation (waterflooding)
$K_{ro,max}$	end-point of the K_{ro} curve	t	time
$K_{rw,max}$	end-point of the K_{rw} curve (at S_{orw})	U	velocity
l	porous medium thickness	γ_{ow}	oil/water interfacial tension ($mN.m^{-1}$)
n	saturation exponent	γ_{og}	oil/gas interfacial tension ($mN.m^{-1}$)
N	number of transmitted photons	γ_{wg}	water/gas interfacial tension ($mN.m^{-1}$)
N_0	number of incident photons	μ	linear absorption coefficient
P	pressure	μ_o, μ_w	oil and water viscosities (Pa.s)
Q	flowrate	ρ_o, ρ_w	oil and water densities ($Kg.m^{-3}$)
r	pore radius	ϕ	porosity
R_t	resistivity of partially saturated rock	<i>Subscripts</i>	
R_0	resistivity of fully saturated rock	pm	porous medium
S	saturation	o	oil
S	spreading coefficient ($mN.m^{-1}$)	g	gas
$S_{i sc,}$ $i=w,o,g$	x-ray CT-scanner determined saturation	w	water

Acknowledgements: The authors wish to thank Mr. P. Bruzzi for his help with the experiments.

References

- 1 Archie, G.E., "The Electrical Resistivity Log as an Aid in Determining Some Reservoir Characteristics", *Trans. AIME*, **146**, 54, 1942.
- 2 Barroux, C., Bouvier, L., Maquignon, P., Thiebot, B. "Alternate Dual-Energy Gamma-Ray Attenuation Technique: A New Tool for Three-Fluid Saturation Measurements in IOR Flood Experiments", 6th European IOR-Symposium, Stavanger, Norway, May 21-23, 1991.
- 3 Chatzis, I., Kantzas, A. and Dullien, F.A.L. "On the Investigation of Gravity Assisted Inert Gas Injection Using Micromodels, Long Berea Sandstone Cores, and Computer Assisted Tomography", Paper SPE 18284, 63rd Annual Conference and Exhibition of the SPE, Houston, TX, October 2-5, 1988
- 4 Foulser R., Naylor, P., Seale, C., "Relative permeabilities for the gravity stable displacement of waterflood residual oil by gas", *Trans IChemE*, **68(A)**, 307-315, 1990
- 5 Hagoort, J. "Oil Recovery by Gravity Drainage", *Society of Petroleum Engineers Journal*, 139-150, June 1980
- 6 Kalaydjian, F. "Performance and analysis of three-phase capillary pressure curves in presence of connate water", Paper SPE 24878, 67th Annual Technical Conference and Exhibition of the SPE, Washington DC, October 4-7, 1992
- 7 Kalaydjian, F., Moulu, J.-C., Vizika, O. and Munkerud P.-K. "Three-Phase Flow in Waterwet Porous Media: Determination of Gas/Oil Relative Permeabilities under Various Spreading Conditions", Paper SPE 26671, 68th Annual Technical Conference and Exhibition of the SPE, Houston TX, October 1993.
- 8 Kalaydjian, F., Tixier, M., "Effect of the spreading coefficient on gas-oil capillary pressure curves in presence of connate water", SCA 9106, SCA Annual Technical Conference, San Antonio, TX, August 21-22, 1991
- 9 Longeron, D.G., Argaud, M.G., Feraud, J.P. "Effect of overburden pressure and the nature and microscopic distribution of fluids on electrical properties of rock samples", SPEFE, 194-202, June 1989.
- 10 Vizika, O., Lombard, J.M. "Wettability and Spreading : Two Key Parameters in Oil Recovery With Three-Phase Gravity Drainage", Paper SPE 28613, 69th Annual Technical Conference and Exhibition, New Orleans, LA, USA, 25-28 Septembre 1994.